Experimental and optimization studies of Ultrasonic assisted friction stir weldments of AA2014-T651 using Graph theory

Suvarna Raju Lam
Borigorla Venu (venuborigorla@gmail.com)
Vignan's Lara Institute of Technology and Science https://orcid.org/0000-0002-1523-2424

Research Article

Keywords: UAFSW, Mechanical Characteristics, Microstructure, Graph Theory, Tool Rotation Speed, Weld Speed

Posted Date: March 25th, 2022

DOI: https://doi.org/10.21203/rs.3.rs-1153295/v1

Experimental and optimization studies of Ultrasonic assisted friction stir weldments of AA2014-T651 using Graph theory

Suvarna Raju Lam[1], Venu Borigorla[2*]

[1] Dept. of Mechanical Engineering, VFSTR (Deemed to be University), Guntur-522213.

[2] Dept. of Mechanical Engineering, VLITS, Guntur-522213.

Corresponding author email: venuborigorla@gmail.com

Abstract

Joining of Al-Cu based alloys such as AA2014-T651 is very difficult by fusion welding techniques due to liquefaction and solidification cracks. Therefore, solid state welding namely Friction Stir Welding (FSW) is most suitable to join these alloys. The main objective of this work is to identify the most influenced process parameters such as rotation speed of the tool, and tool traverse speed and their levels for fabricating the weldments by FSW process with using ultrasonic vibrations (UAFSW). A set of experiments were carried out using the plain cylindrical and taper threaded cylindrical tool pin profile at different levels of process parameters and experimental results were collected. A graph theory and utility concept was proposed and found an optimal working condition for better weldment properties. The UAFSW process enhanced the AA2014-T651 weldment mechanical characteristics at 1100 rev/min of tool rotation speed, and 40 mm/min of tool traverse speed. The tensile strength, yield strength, percentage of elongation, impact strength and micro hardness were found to be 431.69 MPa, 307.47 MPa, 11.66 %, 8.32 J, and 139 HV respectively at optimal working condition. The weld joint obtained using a taper threaded tool pin profiled with ultrasonic vibration exhibits 95% joint efficiency compared to the weldments made by plain cylindrical taper tool pin profile with ultrasonic vibration. The measured characteristics have been correlated with microstructure and fracture features. The optimized responses were verified by the validation test.

Keywords: UAFSW, Mechanical Characteristics, Microstructure, Graph Theory, Tool Rotation Speed, Weld Speed.

1.0 Introduction:

The AA 2014-T651 alloy was developed with a wide range of applications in view, including transportation, aircraft, and applications [1]. The AA2014 is a difficult to weld because of high thermal diffusivity by conventional welding techniques because of

its liquefaction, solidification cracks, hot cracking, and porosity produced after the conventional welding. To overcome these difficulties, friction stir welding (FSW) was developed, in which weld takes place without fusion at the interface of the two parts to be welded and no filler metal is added [2]. During the FSW, the two metal are mixed by the stirring action of rotating tool at plasticization temperature. The heating is accomplished by friction between the workpiece and the tool, which provides the material to soften around the pin. The combination of a tool rotational speed (TRS) and its translation speed deform the material from the front of the pin to the rear of the pin and mixes thoroughly. The material goes through extreme plastic deformation, resulting in significant grain refinement during FSW [3]. Zhang and Zhang [4] reported that increased speeds, including TRS and tool traverse speeds (TTS), can both accelerate the material flow, particularly in front of the pin on the retreating side, where the material flow is quickest [4]. But the mechanical properties of weldments made by conventional FSW do not reach the base metal properties. Therefore, the present study focusing on development of FSW to improve mechanical properties in the weldments.

FSW is a new processing technique, developed by Wayne Thomas at TWI in 1991, UK. It is becoming an emerging technique with its wide area of applications. Compare to conventional welding techniques, it reduced distortion & defect rate, simplifies dissimilar alloy welding, eliminates consumables, and reduces health diseases and hazards and no weld pool [5, 6]. FSW has numerous advantages such as mechanical characteristics enhancement under welding, good protection to the welder, strong in welding, suitable for limited thickness materials [7]. FSW has some shortcomings like a keyhole, heavy-duty clap set, and large axial forces are required [5]. Most importantly, the tool life in FSW of high-temperature materials is significantly reduced. Repeated replacement of worn-out equipment can lead to higher costs of production, resulting in lower production rates and additional costs. Furthermore, the use of damaged equipment presents another problem in terms of welding efficiency [5]. The strength of friction stir weldments was limited is mainly related to the lack of softening of the metal during the welding system [4].

The effect of different pin features and orientation/placement of the materials on the advancing side were investigated for friction stir welding (FSW) of dissimilar aluminum alloys AA2050 and AA6061 are reported by Reza et al. [8] and concluded that quality welds are produced by pin with thread+3 flats at low TRS and TTS. Later, ultrasonic

assisted FSW (UAFSW) was proposed and found enhanced mechanical properties in the weldments with reduced axial welding forces [9,10]. Usage of ultrasonic waves to tool has multiple effects like improving the weld quality, enhance the processing speeds along with a huge decrease in deformation forces [11]. Therefore, the researchers concentrated on implementation of UAFSW for various metals. Ultrasonic vibrations will improve mechanical properties by reducing shear stress and yield stress of materials. Process effectiveness of welding can be improved by ultrasonic vibrations as a supplementary energy to the process [12,13]. Park et al. [14] conducted experiments and concluded that adding of ultrasonic vibrations to FSW in the tool feed direction improved tool life and reduced welding forces. Amini et al. [15] reported that the ultrasonic vibrations improved the tool penetration, which reduces the axial force by about 25% and welding force up to 10%.

Liu et al. [16] carried out UAFSW experiments on AA 2014-T4 at two levels of TRS and TTS with 20Khz frequency and found improved weld quality and mechanical properties of the joint. Moradi et al. [17] conducted UAFSW experiments on dissimilar aluminium alloys AA6061-T6 to AA 2024-T3 and found improved plasticized material flow, eliminated the welding defects and also improved the material bonding strength at joint. As shown in Figure 1, ultrasonic waves are transmitted directly into the workpiece without impacting its exterior of the workpiece. The ultrasonic vibrations exerted to the rotating tool by sonotrode in two directions i.e. axial direction and welding directions. During the UAFSW, the ultrasonic vibrations are directly transferred to the workpiece and eliminates the energy losses [18]. Ultrasonic vibrations exerted into the welding direction was firstly introduced by Park et al. [19] and observed an enhancement of material properties. Ruilin et al. studied effect of the tool traverse speed along with ultrasonic vibrations on the weld quality and concluded that the ultrasonic vibrations are not effective at lower tool traverse speeds [20]. Ji et al., introduced a new ultrasonic vibration system for friction stir welding of Mg and Al alloys and found better mixing of alloys as well as improved the toughness, elongation and tensile strength of the joint [21].

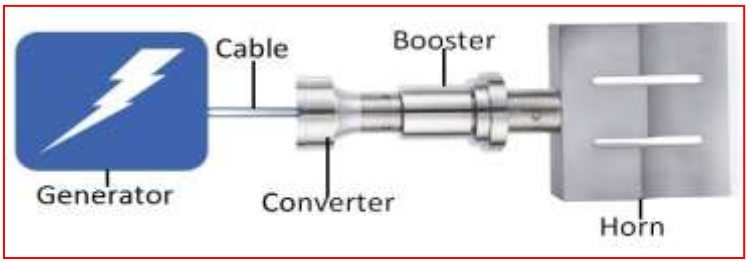

Figure 1 Schematic representation of Ultrasonic Vibration assisted FSW.

Researchers have used different optimization techniques to process parameters optimization to maximize the mechanical characteristics. A conventional approaches like design of experiments, Taguchi method, particle swarm optimization, response surface methodology, grey relation analysis, genetic algorithm, ant colony algorithm, and the multi-objective biogeography-based optimization algorithm are widely used in the FSW process [22,23]. However, the mentioned approaches were not able to achieve better process parameters. To mitigate these troubles, graph theory and utility concepts were developed.

The present study focuses on the process parameters optimization using graph theory and utility concepts to predict the better mechanical characteristics of UAFSW of AA 2014-T651 weldments. To access the process parameters and impact of ultrasonic vibrations on mechanical characteristics of weldments fabricated by FSW.

2.0 Experimental procedure:

The present study is carried out in two phases, in the first stage, the workpieces of AA2014-T651 sizes of 140x60x6 mm were welded by UAFSW. A specially designed tool namely plain cylindrical taper tool (PCT) and taper threaded cylindrical tool pin (TCT) profiles are used to produce strong weldments. The weldment was fabricated at three levels of TRS (700, 900 and 1100 rev/min) and three levels of TTS (40, 50 and 60 mm/min) with 1.5^{o} of constant tool tilt angle. The FSW carried out on vertical milling machine as shown in Figure 2. The machine contains the capacity of 10 hp, spindle speed up to 3000 rpm, and traverse speed of 26 to 60 mm/min. AA2014-T651 friction stir weldments have been successfully fabricated with and without assistance of ultrasonic vibrations (amplitude and frequency are 5µm and 20,000 Hz respectively) with the two tool pin profiles and displayed in Figure 3. The AA2014-T651 manufactured welds are cross-segmented transitionally to the welding direction according to ASTM-E8 and A370 specifications using the wire electrical discharge machining. To test mechanical

characteristics, the samples were cleaned at the surface and edges to prevent stress concentration [23]. Figure 4 displays the schematic diagram for the tensile and Impact

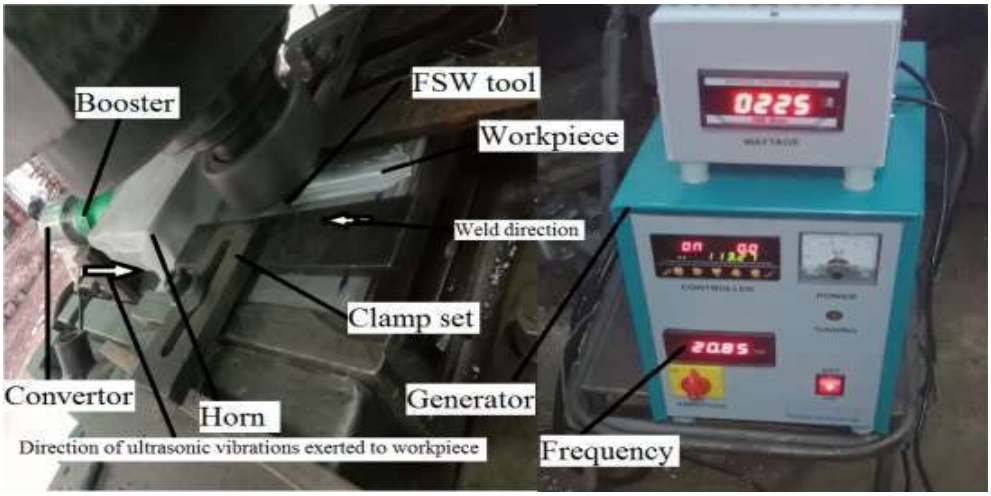

Figure 2 Schematic representation of UVAFSW

Figure 3 Schematic representation of UAFSW weldments (TRS and TTS)
a. 700 rev/min; 40 mm/min, b. 700 rev/min; 50 mm/min, c. 700 rev/min; 60 mm/min, d. 900 rev/min; 40 mm/min, e. 900 rev/min; 50 mm/min, f. 900 rev/min; 60 mm/min, g. 1100 rev/min; 40 mm/min, h. 1100 rev/min; 50 mm/min,and i. 1100 rev/min; 60 mm/min.

specimens. Samples of scale 10x10 mm have been sectioned from stir zone of FSWed specimens for optical metallography. The samples were placed by Bakelite powder with 2 minutes of heating and 6 minutes of cooling time by applying pressure. The specimens were prepared according to the standards of Al alloys and etched with a mixture of 2 ml of HF, 3 ml of HCL, 5 ml of HNO_3, and 190 ml of distilled water for 30-60 seconds to expose the microstructure.

The microhardness was measured at the stir zone using a digital microhardness tester (HVS-100B model). A universal testing machine was used for the tensile test at a crosshead speed of 0.5 mm/min with 100 KN capacity at room temperature. Izod impact tester was used for measuring the weld impact strength.

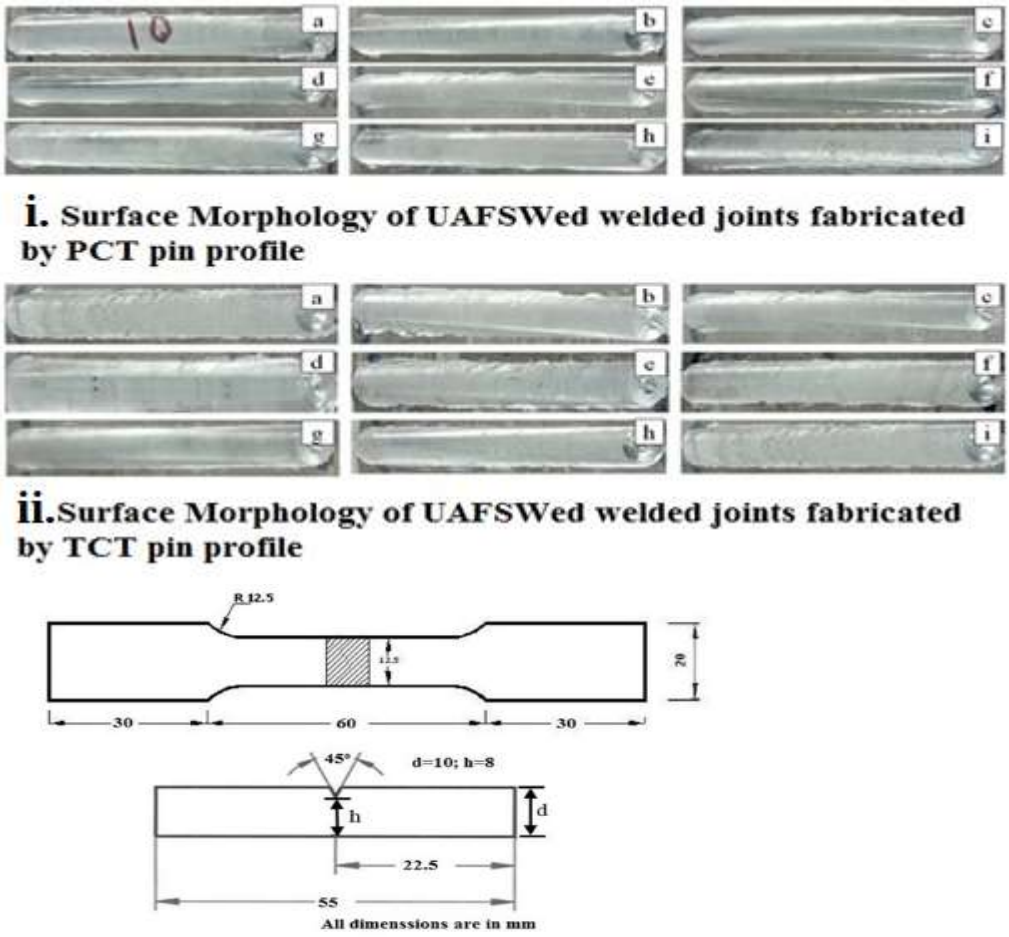

Figure 4 Schematic sketch of Tensile and Impact Specimens

In the second stage, process parameters are optimized to improve mechanical characteristics using graph theory and utility concepts. In this stage, the weights are calculated using the experimental data by keeping the tensile strength (TS), yield strength (YS), percentage of elongation (EL), impact strength (IS), and hardness (H). New process

variables and their corresponding responses are obtained using the utility concept and obtain the best solutions based on the rank.

3.0 Results and Discussion:

The material flow and temperature generation during the weld were influenced by UAFSW process parameters, thereby influencing the microstructural evolution of the material. This microstructural modification of the material leads to the enhancement of characteristics. Since the present study aims to maximize the mechanical characteristics of weldments, the process parameters are optimized by graph theory, and the utility concepts are illustrated in this section.

3.1 Mechanical Characteristics:

The evaluated mechanical characteristics of AA2014-T651 UAFSWed weldments are presented in Table 1. The weldments fabricated by the taper threaded pin profile tool in UAFSW at 1100 rev/min of the rotation speed and 40 mm/min of traverse speed of tool exhibited higher tensile characteristics with a joint efficiency of 95% compared to plain cylinder pin profile tool at various conditions. This is owing to the compressive forging force on the weld, thorough mixing of the material, and also proper material flow due to the influence of ultrasonic vibrations during the welding. Hence, the welds obtained with higher stirring and mixing action of the tool leads to high strength in the stir zone while simultaneously keeping a notable extent of ductility. The percentage of elongation is also higher in the weldments fabricated with a threaded taper cylindrical tool pin profile compared to a plain taper cylindrical profiled tool pin. This may be due to the increased resistance to deformation of the welded weldments which is due to the microstructural changes in the stir zone.

In FSW, the material flow on the upper side of the friction stir weld can be accelerated by the shoulder. The material in the nugget zone can be more completely mixed by increasing the angular velocity of the pin, which enhances the joining quality of the two welding plates. Increased speeds, including rotational and translational speeds, can both accelerate the material flow, particularly in front of the pin on the retreating side, where the material flow is quickest, which results in improved mechanical properties [4]. The mechanical characteristics are evaluated in different stages of FSW (i.e. base metal, plain taper cylindrical profile tool without ultrasonic vibration, taper threaded cylindrical profile tool without ultrasonic vibration, plain taper cylindrical profile tool with ultrasonic

vibration and taper threaded cylindrical profile tool with ultrasonic vibration) and are presented in Table 2.

The material around the pin is considerably softer with the application of ultrasonic vibration and can withstand reasonable plastic deformation due to the acoustic elastic effect, resulting in the formation of lamellar structures alternating from fine grain and coarse grain. The breakdown of metastable platelets and their re-precipitation appear in SZ [24]. In UAFSW, formation of fine grain structure in the stir zone is attributable to dynamically recrystallization and thermal exposure. Because of the intense heat generated while processing, the material attains the plastic state. The tool stirring action on the metal in the stir zone disintegrate the coarse and elongated grains into smaller grains. Hence refined microstructure is found along with the enhanced mechanical properties. Therefore, the mechanical properties in the weldments are found to be closed to base metal properties.

Table 1 Mechanical characteristics of friction stir AA2014 weldments with ultrasonic vibrations.

Tool pin profile	TRS (rev/min)	TTS (mm/min)	TS (MPa)	YS (MPa)	EL (%)	IS (J)	H (HV)	Joint strength (%)
PCT tool pin profile	700	40	329.67	269.73	9.10	7.57	111	68
	700	50	313.02	266.40	8.51	6.80	108	64
	700	60	296.37	263.07	7.91	6.04	105	61
	900	40	344.10	270.84	9.09	7.68	114	71
	900	50	327.45	267.51	8.52	6.92	112	67
	900	60	310.80	265.29	7.96	6.16	109	64
	1100	40	357.42	271.95	9.14	7.80	117	73
	1100	50	340.77	269.73	8.61	7.05	115	70
	1100	60	324.12	266.40	8.01	6.29	113	67
TCT tool pin profile	700	40	370.74	284.16	8.66	6.76	129	76
	700	50	341.88	238.65	7.55	6.03	125	70
	700	60	313.02	194.25	6.55	5.30	122	64
	900	40	379.16	295.26	10.10	7.59	133	78
	900	50	366.30	250.86	9.10	6.86	130	75
	900	60	338.55	206.46	7.99	6.24	126	69

	1100	40	431.69	307.47	11.66	8.32	139	95
	1100	50	392.94	263.07	10.66	7.80	136	81
	1100	60	364.08	217.56	9.55	7.07	131	75
Base metal			485	413	13	9	155	

Table 2 Mechanical characteristics of friction stir welded AA2014-T651 fabricated by PCT and TCT with and without ultrasonic vibrations.

Weld condition	**TS (MPa)**	**YS (MPa)**	**%EL**	**Micro Hardness (HV)**	**Impact toughness (J)**
PCT without ultrasonic vibration	322	245	8.23	109	7.5
TCT without ultrasonic vibration	379	277	10.5	129	8
PCT with ultrasonic vibration	357	271	9.14	117	7.8
TCT with ultrasonic vibration	431	307	11.6	139	8.3
Base metal	483	414	13	155	9

The microhardness values of the base metal and the UAFSW weldments are presented in Table 1. The maximum value of hardness is 139 HV obtained at the stir zone (SZ) for the weldments fabricated by threaded taper pin profile tool at 1100 rev/min as the rotation speed of a tool and 40 mm/min as tool traverse speed due to grain refining through dynamic recrystallization [25] and influence of ultrasonic vibrations. The UAFSW joint hardness values of two tool pin profiles are displayed in Figure 5. From the hardness survey, from both sides i.e. retreating and advanced of the HAZ, TMAZ, and SZ were provided. The transition between HAZ and TMAZ obtain a minimum value of hardness due to grain refining through dynamic recrystallization and the influence of ultrasonic vibrations [25,26].

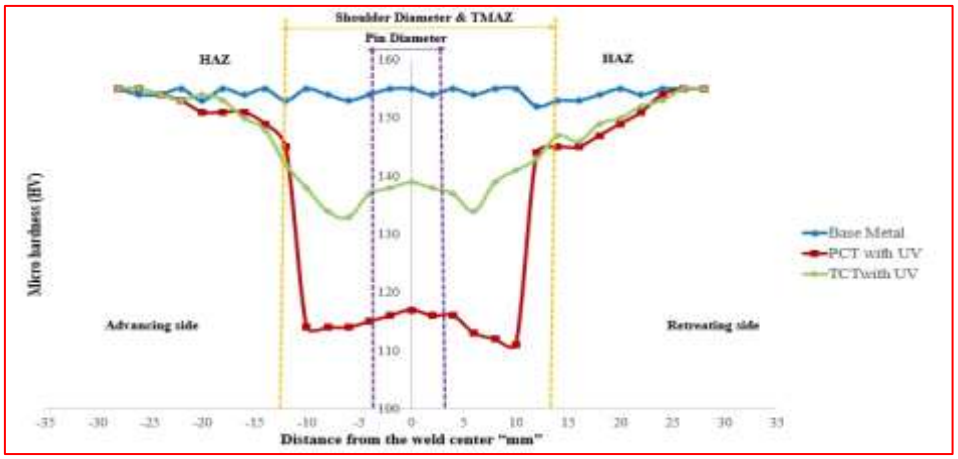

Figure 5 Microhardness distribution of UAFSW weldments for PCT and TCT

3.2 Microstructure:

The microstructures of the weldments were examined at the weld region of friction stir weldments using taper cylindrical tool pin profile and without ultrasonic vibration. The inconsistency revealed significantly unique microstructure in the SZ produced by plain taper cylindrical and taper threaded profile tool with ultrasonic vibration as shown in Figures 6 and 7. It is experimental that the weldments fabricated by the TCT [Figure 7 (g).] resulted in a high reduction in the size of grains and the formation of equiaxed grains in the weldments [27]. This is due to the frictional force exerted, severe stirring action by the friction stir tool, optimum heat generation with the influence of ultrasonic vibrations, and the friction-dominated flow of material was observed [18] at the microstructure which leads to the formation of fine aluminum grains at the SZ. Whereas the weldments produced TCT profile showed equiaxed and finer grains with 4.11μm of mean grain size, at weld nugget by tool traverse speed of 40 mm/min and TRS of 1100 rev/min. Here, ultrasonic vibrations influenced the process which attributes to the greater straining of the metal resulting from process parameters, which causes more strain-free nucleation sites, providing sufficient frictional heating in the SZ. The good stirring action between the tip and collar, and avoids the turbulence which resulted in better mechanical characteristics of the joint. The weldments made by PCT with UAFSW resulted in a great reduction of 5.05 μm in the size of grains which is less than the welded samples at the SZ of the PCT at the same condition. This is due to better mixing of material and finest heat generation due to the influence of ultrasonic vibrations.

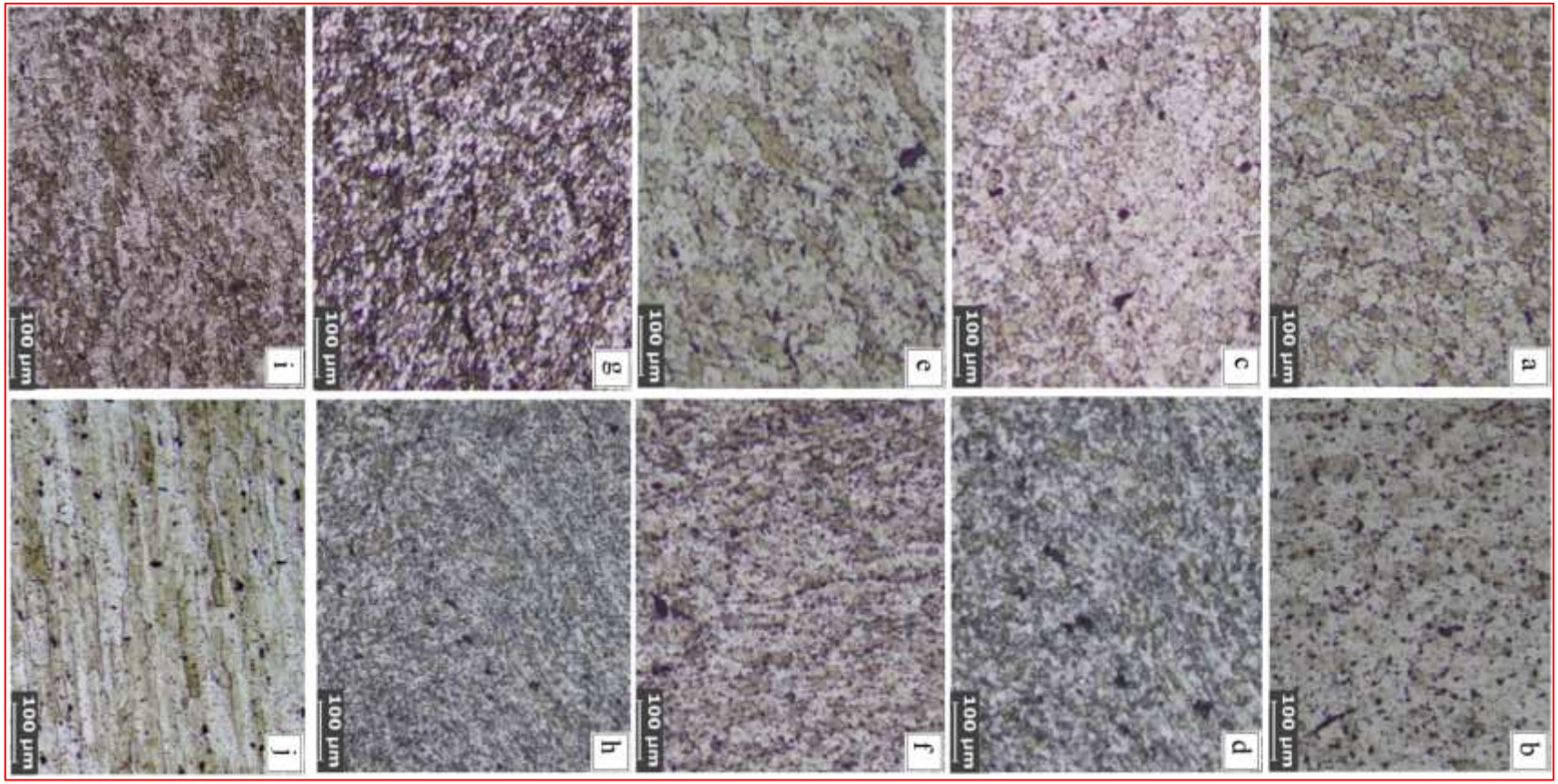

Figure 6 Microstructures of weldments fabricated by UAFSW with PCT a. 700 rev/min; 40 mm/min, b. 700 rev/min; 50 mm/min, c. 700 rev/min; 60 mm/min, d. 900 rev/min; 40 mm/min, e. 900 rev/min; 50 mm/min, f. 900 rev/min; 60 mm/min, g. 1100 rev/min; 40 mm/min, h. 1100 rev/min;50 mm/min, i. 1100 rev/min; 60 mm/min, and j) base metal.

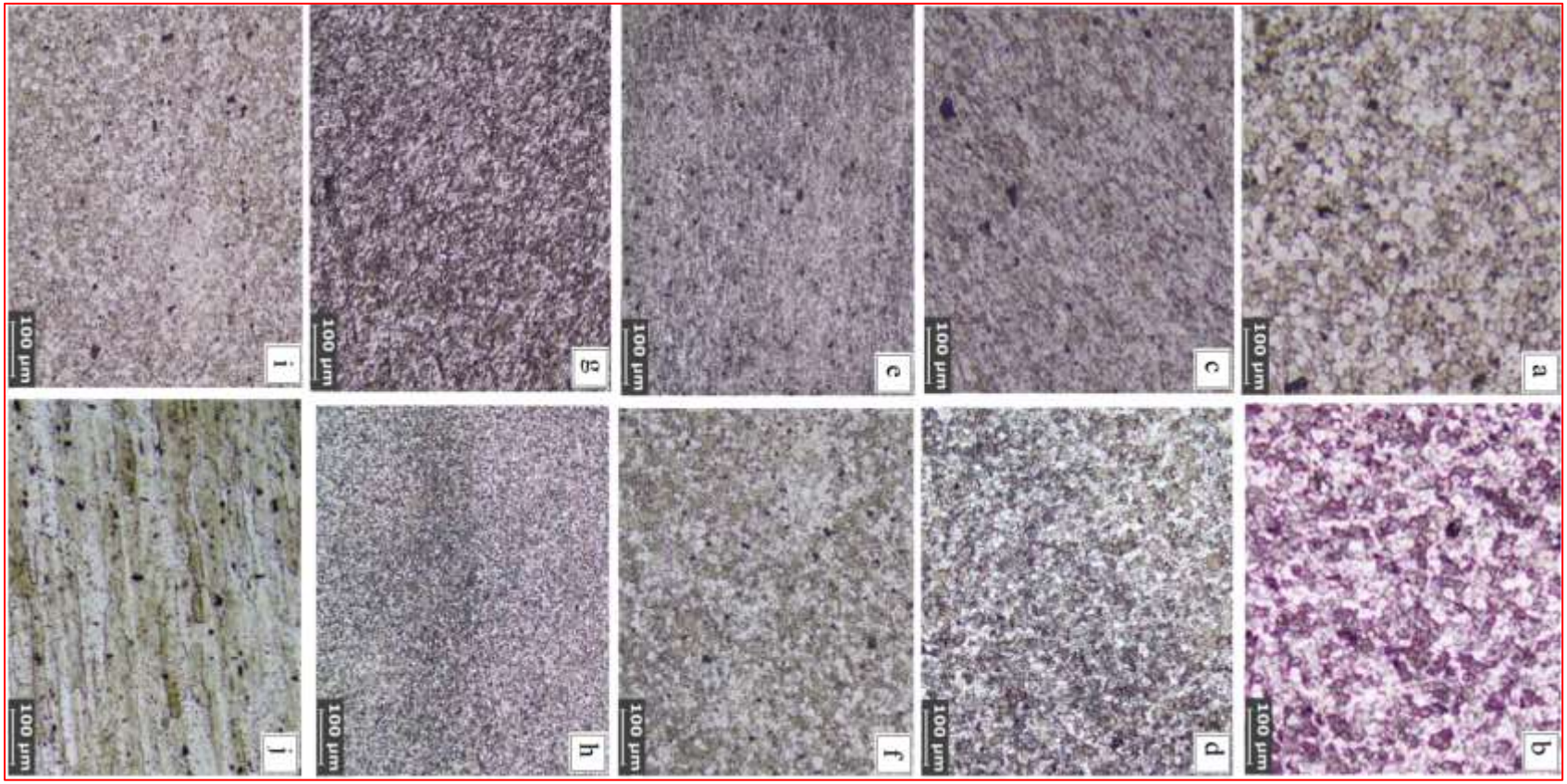

Figure 7 Microstructures of weldments fabricated by UAFSW with TCT a. 700 rev/min; 40 mm/min, b. 700 rev/min; 50 mm/min, c. 700 rev/min; 60 mm/min, d. 900 rev/min; 40 mm/min, e. 900 rev/min; 50 mm/min, f. 900 rev/min; 60 mm/min, g. 1100 rev/min; 40 mm/min, h. 1100 rev/min;50 mm/min, i. 1100 rev/min; 60 mm/min, and j) base metal.

3.2 Fractography:

Fracture surface analysis of tensile specimens of the UAFSW of AA2014-T651 weldments made by different tools such as PCT and TCT pin profiles with different rotation speeds and tool traverse speeds of the tool were shown in Figures 8 and 9. During the tensile test, the specimens were fractured where the hardness value is the lowest i.e. retreating side, which was also examined with the hardness measurement [25]. Weldments made by taper threaded pin profile tool with ultrasonic vibrations exhibited superior ductility (Figure 9 (g).) as compared with the weldments made by plain taper tool pin profile with ultrasonic vibrations. This is because of the presence of small shallow dimples furthermore some huge dimples that resulted in micro dimples coalescence. It could be attributed to the high plastic deformation which indicates a more intense ductile fracture.

Fracture surface analysis of impact specimens of the UAFSW of AA2014-T651 weldments made by PCT and TCT with different TRS and TTS was shown in Figures 10 and Figure 11. The impact fracture surface of a taper threaded tool pin profile [Figure 11 (g).] shows large and fine dimples, which could be attributed to the better impact strength of the weldments.

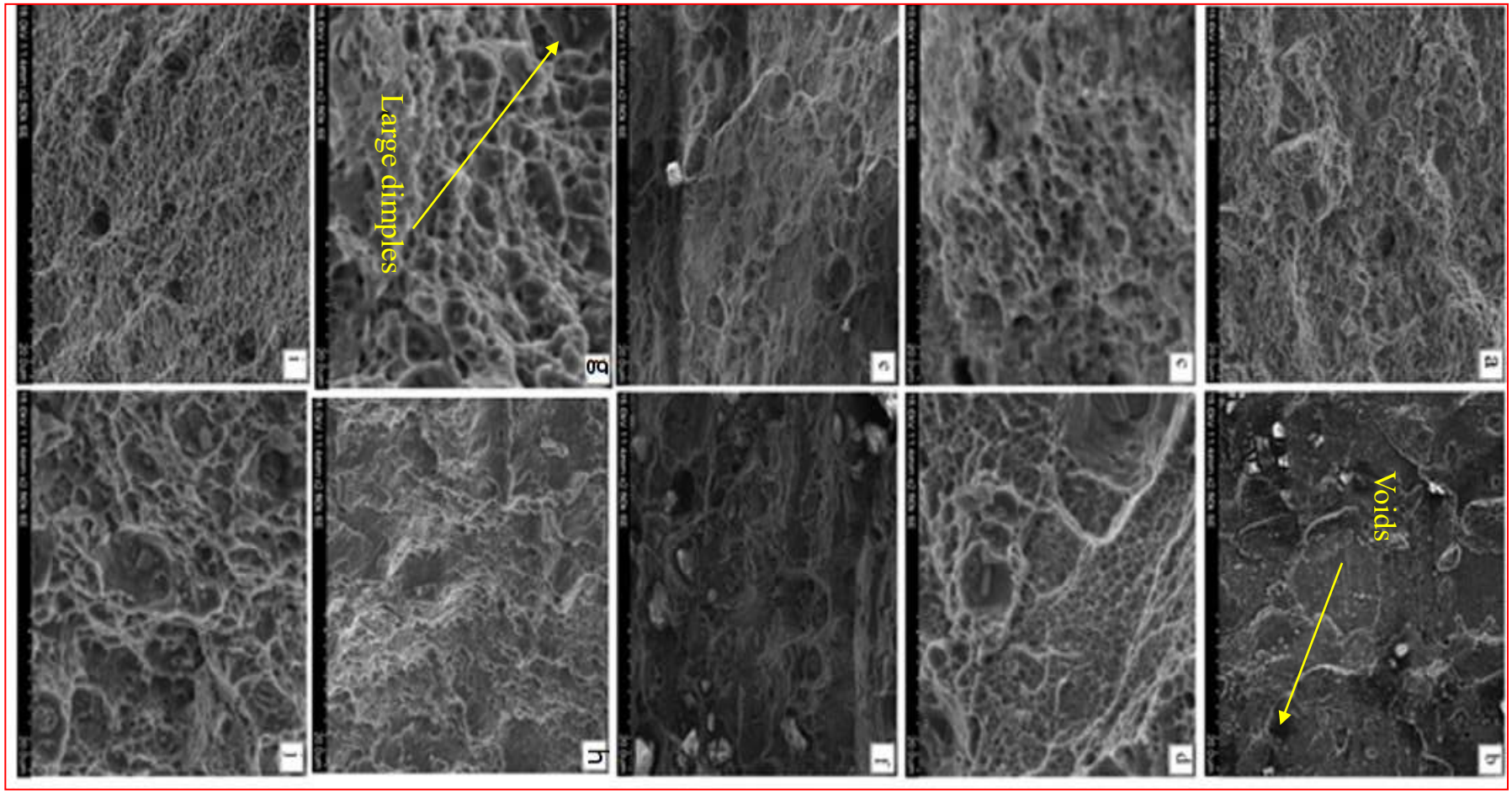

Figure 8 Fracture surface resultant from tensile test of UAFSW with PCT: a. 700 rev/min; 40 mm/min, b. 700 rev/min; 50 mm/min, c. 700 rev/min; 60 mm/min, d. 900 rev/min; 40 mm/min, e. 900 rev/min; 50 mm/min, f. 900 rev/min; 60 mm/min, g. 1100 rev/min; 40 mm/min, h. 1100 rev/min;50 mm/min, i. 1100 rev/min; 60 mm/min, and j) base metal.

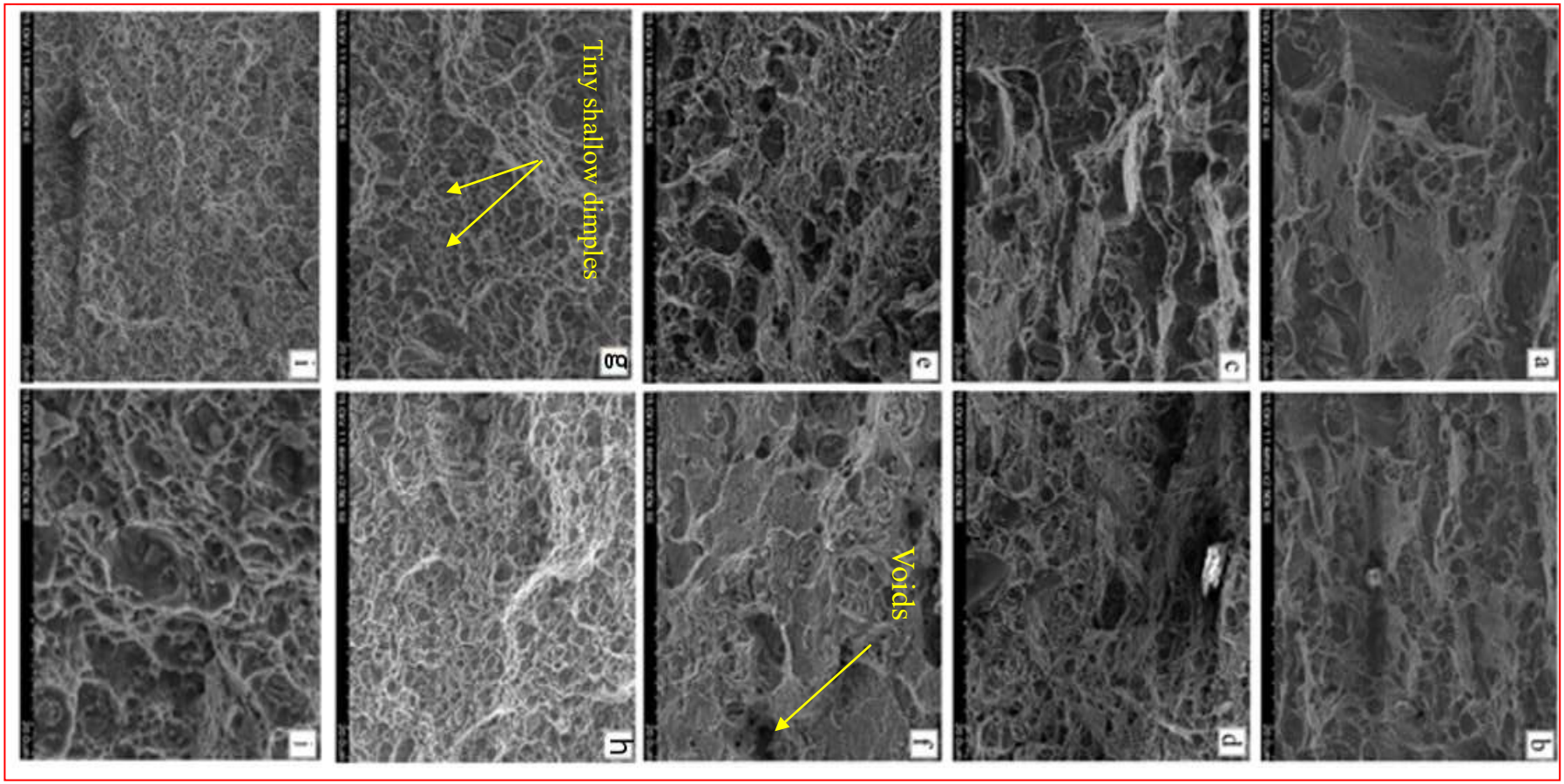

Figure 9 Fracture surface resultant from tensile test of UAFSW with TCT: a. 700 rev/min; 40 mm/min, b. 700 rev/min; 50 mm/min, c. 700 rev/min; 60 mm/min, d. 900 rev/min; 40 mm/min, e. 900 rev/min; 50 mm/min, f. 900 rev/min; 60 mm/min, g. 1100 rev/min; 40 mm/min, h. 1100 rev/min;50 mm/min, i. 1100 rev/min; 60 mm/min, and j) base metal.

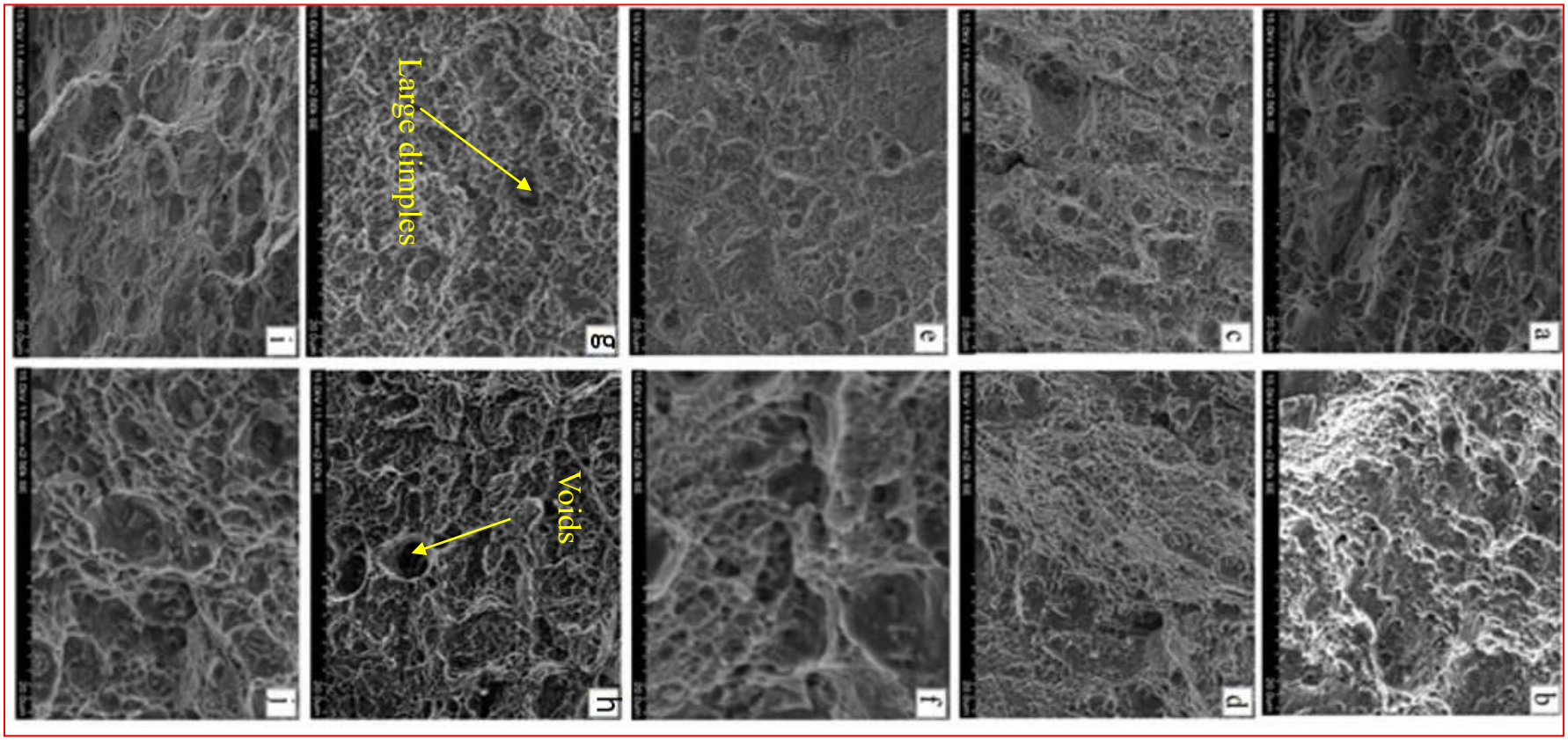

Figure 10 Fracture surface resultant from impact test of UAFSW with PCT: a. 700 rev/min; 40 mm/min, b. 700 rev/min; 50 mm/min, c. 700 rev/min; 60 mm/min, d. 900 rev/min; 40 mm/min, e. 900 rev/min; 50 mm/min, f. 900 rev/min; 60 mm/min, g. 1100 rev/min; 40 mm/min, h. 1100 rev/min;50 mm/min, i. 1100 rev/min; 60 mm/min, and j) base metal.

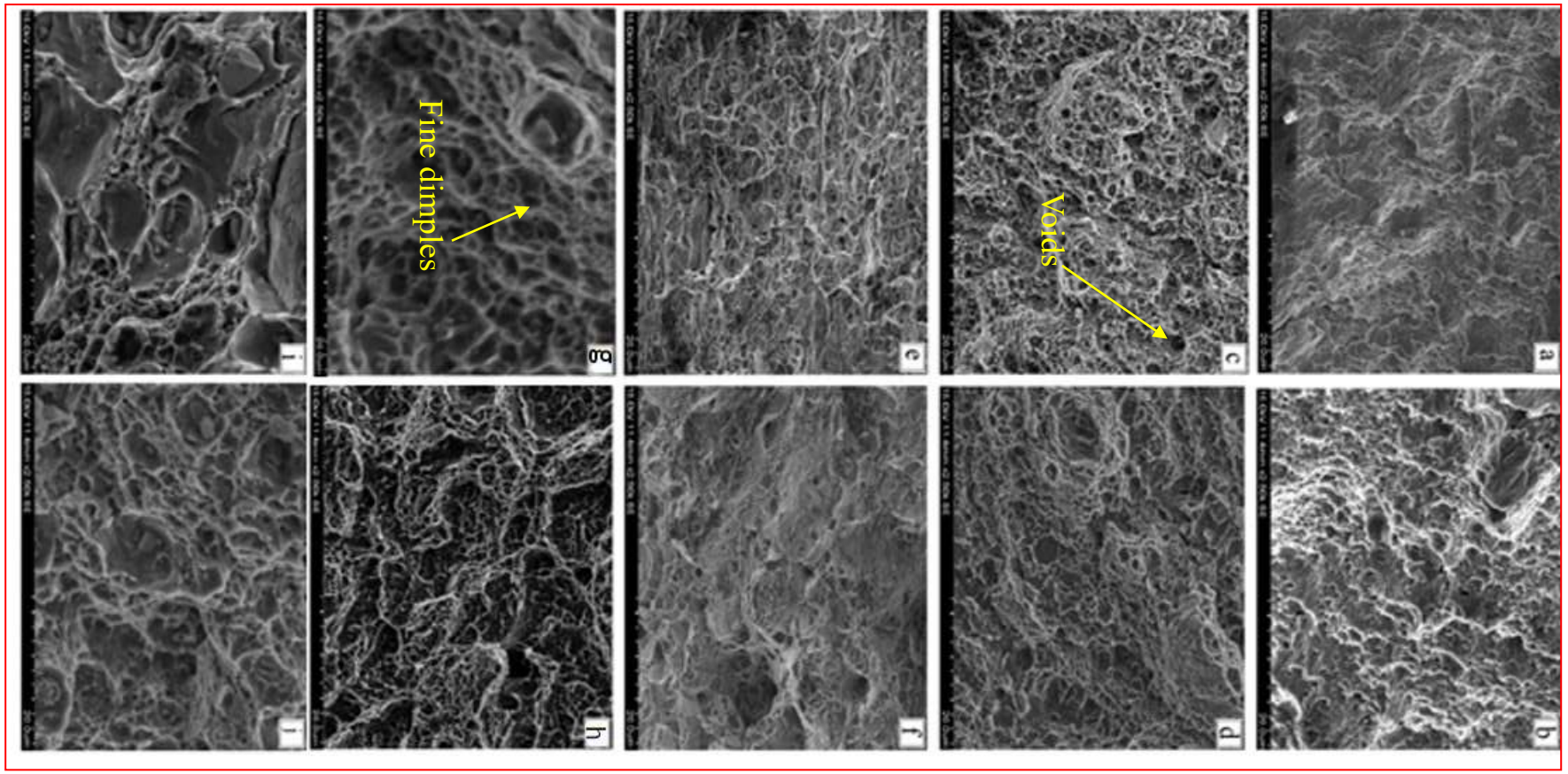

Figure 11 Fracture surface resultant from impact test of UAFSW with TCT: a. 700 rev/min; 40 mm/min, b. 700 rev/min; 50 mm/min, c. 700 rev/min; 60 mm/min, d. 900 rev/min; 40 mm/min, e. 900 rev/min; 50 mm/min, f. 900 rev/min; 60 mm/min, g. 1100 rev/min; 40 mm/min, h. 1100 rev/min;50 mm/min, i. 1100 rev/min; 60 mm/min, and j) base metal.

3.4 Optimization:

In the second phase, the process parameters were optimized by graph theory and utility concept to maximize the mechanical characteristics of weldments, and.

3.4.1. Graph theory algorithm:

Weights to the mechanical characteristics are calculated using six steps.

Step 1: preference graph based on client

A preference graph is developed from the assessments of various investigations and manufacturers [28]. As displayed in Fig. 12, the assessments of five distinct clients are gathered. Based on the assessments of the clients, the characteristics are given priority from high to low as follows:

i. The first client has given topmost priority to the hardness value and followed by the values of impact strength, percentage of elongation, yield strength, and tensile strength.
ii. The second client has given high priority to the values of yield strength and percentage of elongation equally followed by the tensile strength, impact strength, and hardness values.
iii. The third client has given topmost priority to yield strength and percentage of elongation characteristics equally followed by tensile strength, hardness, and impact strength characteristics.
iv. The fourth client has given high priority to the percentage of elongation followed by yield strength, impact strength, tensile strength, and hardness.
v. The fifth client has given high priority to hardness followed by the percentage of elongation, yield strength, tensile strength, and impact strength.

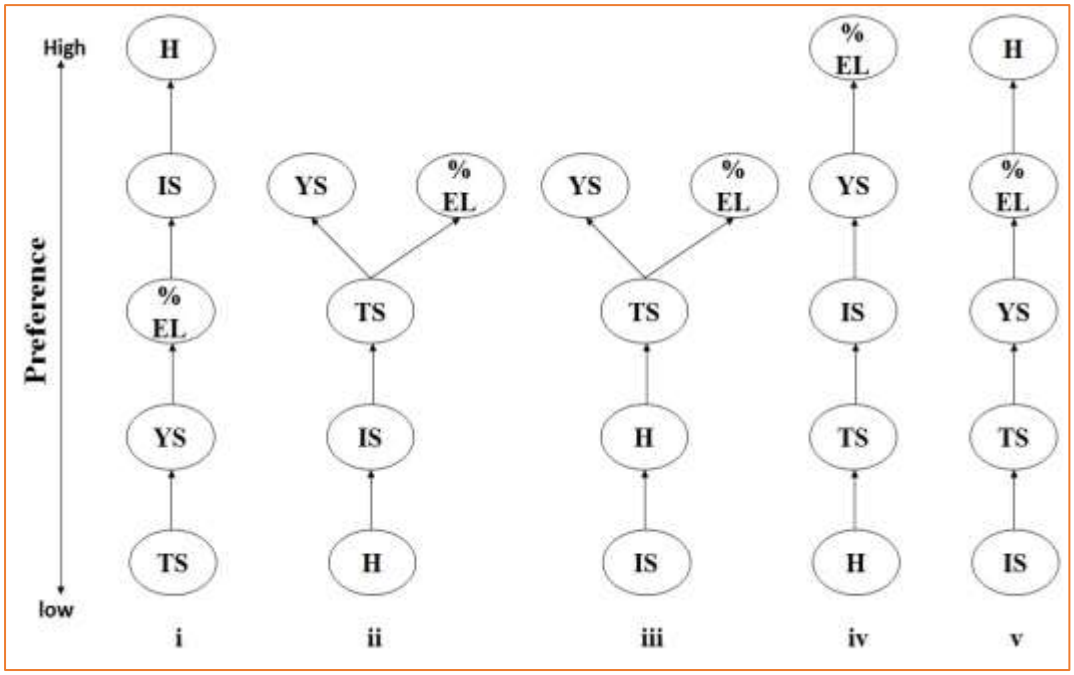

Figure 12 Different user's performance on mechanical characteristics

Step 2: Matrix of Preference:

The transpose of the coefficient matrix is constructed and presented below according to preference graphs.

$$PG_n = [pg_{ij}]_{MxM} \text{ ---------- (1)}$$

Where the client's count was represented with n, and Responses represented with M, and pg_{ij} gives the dominance of i over j in an MxM.

$$PG_1 = \begin{array}{c} \begin{array}{ccccc} \text{TS} & \text{YS} & \text{\% EL} & \text{IS} & \text{H} \end{array} \\ \begin{pmatrix} 0 & 0 & 0 & 0 & 0 \\ 1 & 0 & 0 & 0 & 0 \\ 0 & 1 & 0 & 0 & 0 \\ 0 & 0 & 1 & 0 & 0 \\ 0 & 0 & 0 & 1 & 0 \end{pmatrix} \end{array} \begin{array}{c} \\ \text{TS} \\ \text{YS} \\ \text{\% EL} \\ \text{IS} \\ \text{H} \end{array}$$

$PG_2 =$

	TS	YS	% EL	IS	H	
	0	0	0	1	0	TS
	1	0	0	0	0	YS
	1	1	0	0	0	% EL
	0	0	0	0	1	IS
	0	0	0	0	0	H

$PG_3 =$

	TS	YS	% EL	IS	H	
	0	0	0	0	1	TS
	1	0	0	0	0	YS
	1	0	0	0	0	% EL
	0	0	0	0	0	IS
	0	0	0	1	0	H

$PG_4 =$

	TS	YS	% EL	IS	H	
	0	0	0	0	1	TS
	0	0	0	1	0	YS
	0	1	0	0	0	% EL
	1	0	0	0	0	IS
	0	0	0	0	0	H

$PG_5 =$

	TS	YS	% EL	IS	H	
	0	0	0	1	0	TS
	1	0	0	0	0	YS
	0	1	0	0	0	% EL
	0	0	0	0	0	IS
	0	0	1	0	0	H

Step 3: Dominance matrix (D.:

Among all the performance characteristics more preferred performance characteristics were identified by the D matrix.

$$D^n = PG_n^1+PG_n^2+PG_n^3+PG_n^4+PG_n^5+\ldots.+ PG_n^{M-1}$$

Also,

$$d^n{}_{m=}\sum_{j=1}^{M} pg_{ij} \qquad \text{----------} \quad (2)$$

Where the client's count was represented with n, and Responses represented with M.

The D matrix was calculated using the equation (2), where m value was taken as 5 then:

D_{pg1}	0	0	0	0	0	D_{pg2}	0	0	0	1	1	D_{pg3}	0	0	0	0	1
	1	1	1	1	0		1	0	0	1	1		1	0	0	1	1
	0	1	1	1	0		1	0	0	1	1		1	0	0	1	1
	0	0	1	1	0		0	0	0	0	1		0	0	0	0	0
	0	0	0	1	0		0	0	0	0	0		0	0	0	1	1

D_{pg4}	0	0	0	0	1	D_{pg5}	0	0	0	1	0
	0	0	0	1	1		1	1	1	1	0
	0	1	0	1	1		0	1	1	1	0
	1	1	0	1	1		0	0	0	0	0
	0	0	0	0	0		0	0	1	1	0

Step 4: Relative degree of performance (RDP)

The RDP addresses represent relative assessment among the five mechanical characteristics of a similar preference graph between 0 and 1. The RDP was controlled by utilizing condition (3).

$$RDP^{n}{}_{m} = \frac{1+dm^{n}}{Maxm=1.....M^{1}+d^{n}{}_{m}} \text{ ---------- (3)}$$

	D_{pg1}					RDP_1		D_{pg2}					RDP_2		D_{pg3}					RDP_3
R_{Dpg1}	0	0	0	0	0	0.2	R_{Dpg2}	0	0	0	1	1	0.75	R_{Dpg3}	0	0	0	0	1	0.5
	1	1	1	1	0	1		1	0	0	1	1	1		1	0	0	1	1	1
	0	1	1	1	0	0.8		1	0	0	1	1	1		1	0	0	1	1	1
	0	0	1	1	0	0.6		0	0	0	0	1	0.5		0	0	0	0	0	0.25
	0	0	0	1	0	0.2		0	0	0	0	0	0.25		0	0	0	1	1	0.75

	D_{pg4}					RDP_4		D_{pg5}					RDP_5
R_{Dpg4}	0	0	0	0	1	0.4	R_{Dpg5}	0	0	0	1	0	0.4
	0	0	0	1	1	0.6		1	1	1	1	0	1
	0	1	0	1	1	0.8		0	1	1	1	0	0.8
	1	1	0	1	1	1		0	0	0	0	0	0.2
	0	0	0	0	0	0.2		0	0	1	1	0	0.6

Step 5: Relative Importance Rating (RIR):

The RIR was determined by joining the five mechanical characteristics of RDPs utilizing the underneath equation (4).

$$RIR_m = \frac{\sum_{n=1}^{N} rdp_m{}^n}{Max\ m=1.....M \sum_{n=1}^{N} rdp^n{}_m} \quad \text{---------- (4)}$$

	1	2	3	4	5	Sum
RDP_1	0.2	1	0.8	0.6	0.2	2.8
RDP_2	0.75	1	1	0.5	0.25	3.5
RDP_3	0.5	1	1	0.25	0.75	3.5
RDP_4	0.4	0.6	0.8	1	0.2	3
RDP_5	0.4	1	0.8	0.2	0.6	3

RIR_1= 2.8/3.5 = 0.8; RIR_2=3.5/3.5 = 1; RIR_3=3.5/3.5 = 1; RIR_4=3/3.5 = 0.85; RIR_5=3/3.5 = 1.

	1	2	3	4	5	Sum
RIR	0.8	1	1	0.85	0.85	4.5

Step 6: Weight of responses (W):

Weights of five responses are calculated as follows:

$$W_m = \frac{RIR_M}{\sum_{m=1}^{M} RIR_m} \quad \text{---------- (5)}$$

$W_1 = \frac{0.8}{4.5} = 0.1777$; $W_2 = \frac{1}{4.5} = 0.2222$; $W_3 = \frac{1}{4.5} = 0.2222$; $W_4 = \frac{0.85}{4.5} = 0.1888$; $W_5 = \frac{0.85}{4.5} = 0.1888$.

Then the weights of responses such as TS, %EL, YS, IS, and H are calculated as 0.1777, 0.2222, 0.2222, 0.1888, and 0.1888 respectively.

W_m = (0.17777, 0.2222, 0.2222, 0.1888, 0.1888)

3.4.2 Utility concept:

In the utility concept method the experimental results, preference scales, and weights using to estimate the utility value. This was calculated for five responses for the 9 readings using the below condition.

$$\text{“}U(n,y) = P_{TS}(n,y)*W_{TS} + P_{YS}(n,y)*W_{YS} + P_{\%EL}(n,y)*W_{\%EL} + P_{IS}(n,y)*W_{IS} + P_H(n,y)*W_H\text{”} \quad \text{---------- (6)}$$

Where the pass number is indicated with n and the repetition number is indicated with y. Similarly, W is the weight, and the preference scale was represented with P.

The utility value of all mechanical characteristics was evaluated using the following equation (7), here a preference scale is mandatory. The "P-value was chosen as 0 to 9 based on the acceptable level".

$$P = A \log \frac{x^i}{x_j{}^i} \quad \text{---------- (7)}$$

Where the value attribute response is the value of x^i, the maximum acceptable value is x^i_j of mechanical characteristics and A is the constant. In this work, the maximum acceptable levels for TS, YS, %EL, IS, and H are taken as 431.69 MPa, 307.47 MPa, 11.66 %, 8.32 J, and 139 HV respectively. The five responses of attributes are estimated using MINITAB 2019. Preference scales for the mechanical characteristics are calculated as follows:

Preference scale for tensile strength (TS):

$$P_{TS} = -184.52 \log \frac{X_{TS}}{483} \quad \text{---------- (8)}$$

Preference scale for yield strength (YS):

$$P_{YS} = -69.66 \log \frac{X_{YS}}{414} \quad \text{---------- (9)}$$

Preference scale for percentage of elongation (%EL):

$$P_{\%EL} = -190.49 \log \frac{X_{\%EL}}{13} \quad \text{---------- (10)}$$

Preference scale for impact strength (IS):

$$P_{IS} = -266.59 \log \frac{X_{IS}}{9} \quad \text{---------- (11)}$$

Preference scale for yield strength (YS):

$$P_{H} = -190.20 \log \frac{X_{YS}}{155} \quad \text{---------- (12)}$$

Overall utility value for taper threaded cylindrical tool pin profile was calculated using equation (6) and presented in Table 3.

From Table 3, one best combination of the process parameters, which is having the first rank is selected as the optimum combination of TRS and TTS. Based on these combinations, setup experiments were done for validation of the process.

Similarly, the graph theory and utility concept was implemented for the plain cylindrical tool pin profile. However, the TCT profile with ultrasonic vibrations exhibits better mechanical characteristics compared to the PCT profile.

Table 3: Utility values of the threaded taper cylindrical tool pin profile with ultrasonic vibrations:

S.-No.	TRS (rpm)	TTS (mm/min)	TS (MPa)	YS (Mpa)	% EL	IS (J)	H (HV)	Utility value	Rank
1	700	40	370.74	284.16	8.66	6.76	129	22.5163	6
2	700	50	341.88	238.65	7.55	6.03	125	30.2076	8
3	700	60	313.02	194.25	6.55	5.3	122	38.4930	9
4	900	40	379.16	295.26	10.1	7.59	133	16.2523	3
5	900	50	366.3	250.86	9.1	6.86	130	22.1922	5
6	900	60	338.55	206.46	7.99	6.24	126	29.4511	7
7	1100	40	431.69	307.47	11.66	8.32	139	8.9145	1
8	1100	50	392.94	263.07	10.66	7.8	136	14.6186	2
9	1100	60	364.08	217.56	9.55	7.07	131	21.6090	4

4.0 Validation of optimization:

To check the responses the validation experiment is carried out at an optimal combination of TRS and TTS. The normal utility value predicted at the optimal combination of the TRS and the TTS was found to be 8.9145 and it is within the anticipated range of 500 rpm to 1500 rpm of tool rotation speed, and 30 mm/min to 70 mm/mins. The five responses were also predicted at the same optimal combination of process parameters. The anticipated values and experimental values of the five responses were well fit within the anticipated optimal range by a 99% of R-Sq value.

5.0 Conclusions:

In the present study, influence of process parameters such as rotation speed of the tool, and tool traverse speed and ultrasonic vibration on mechanical properties of weldments was studied. The work was done in two stages: in the first stage, the experiment was carried out using ultrasonic vibration, and in the second stage, the process parameters were optimized using graph theory and utility concept. From the investigation the following important conclusions have been derived:

- AA2014-T651 friction stir weldments have been successfully fabricated with assisting of ultrasonic vibrations with the PCT and TCT.
- Weldments fabricated by a PCT at a TRS of 1100 rev/min, TTS of 40 mm/min exhibited superior mechanical characteristics. This is due to the compressive

forging force on the weld, thorough mixing of the material, and also proper material flow due to the influence of ultrasonic vibrations during the welding.

- The weld joint obtained using a TCT with ultrasonic vibration possesses 95% of joint efficiency compared to the weldments made by PCT with ultrasonic vibration.
- The microstructure at the stir zone of UAFSW weldments using a TCT contain fine grains. This is due to the influence of ultrasonic vibrations which attributes to the higher straining of the metal resulting from process parameters, which causes more strain-free nucleation sites, provides sufficient frictional heating in the SZ.
- The highest hardness value of 139 HV has been observed at the SZ of the weldments fabricated by a TCT compared to the PCT. This is due to grain refining through dynamic recrystallization and the influence of ultrasonic vibrations.
- Using graph theory weights for TS, YS, %EL, IS and H are evaluated as 0.1777, 0.2222, 0.2222, 0.1888, and 0.1888 respectively using graph theory. The graph theory and utility concept optimized the process parameters as 1100 rpm of TRS and 40 mm/min of TTS.
- The predicted values and experimental values of the mechanical characteristics were well fit within the predicted optimal range by 99% of the R-Sq value.

Acknowledgment

The authors are very much thankful to the authorities of SERB/F/11385/2018-2019 for granting funds to this project and Vignan's Deemed to be university, for extending the facilities to complete the project work.

Declarations:

a. Funding:

This work was supported by Department of Science and technology, Govt. of India (Sanction no. SERB/F/11385/2018-2019)

b. Conflicts of interest/Competing interests:

Conflict of Interest for all authors is None.

c. Availability of data and material:

The data supporting the findings of this study are available within the article.

d. Code availability:

Not applicable

e. Ethics approval:

Not applicable

f. Consent to participate:

Not applicable

g. Consent for publication:

Not applicable

h. Authors' contributions:

Dr. L Suvarna Raju and Dr. B Venu have defined the objectives of the present study and experimental plan. Dr. B Venu carried out experimentation and collected experimental results, Dr. L Suvrna Raju has studied microstructural and mechanical characteristics and both the authors have involved in optimization and preparation of manuscript.

References:

1. Rajendran C, Srinivasan K, Balasubramanian V, Balaji H, Selvaraj P. (2019) Effect of tool tilt angle on strength and microstructural characteristics of friction stir welded lap joints of AA2014-T6 aluminum alloy. Trans Nonfer Met Soc of China 29(9):1824-1835.

2. Kah P, Rajan R, Martikainen J, Suoranta R (2015) Investigation of weld defects in friction-stir welding and fusion welding of aluminium alloys. Int J Mech Mat Eng 26: 1-10.

3. Padhy GK, Wu CS, Gao S (2018) Friction stir based welding and processing technologies - processes , parameters , microstructures and applications : A review. J Mat Sci & Tech 34:1–38.

4. Zhang Z, Zhang HW (2007) Material behaviors and mechanical features in friction stir welding process. Int J Adv Manuf Technol 35:86–100.

5. Threadgill PL, Leonard AJ, Shercliff HR, Withers PJ (2009) Friction stir welding of Al alloys. Int Mater Rev 54(2): 49–93.

6. Venu B, Bhavya swathi I, Raju LS, Santhanam G (2019) A Review on Friction Stir Welding of various metals and its variables. Mat Today Proc 18:298-302.

7. Yadav VD, Bhatwadekar G (2014) Friction stir welding of dissimilar materials between AA6101 Al and pure copper. Int J Eng Sci Res Tech 3(12): 505–508.

8. Reza-E-Rabby Md,Tang W, Reynolds AP (2015) Effect of tool pin features on process response variables during friction stir welding of dissimilar aluminum alloys. Sci and Tech Welding and Joining 20(5):425-432.

9. Ding W, Kumar S, Wu CS, Padhy GK (2017) Application of ultrasonic vibrations in welding and metal processing: A status review. J Manuf Proc 26: 295-322.
10.Lai R, He DQ, Liu L, Ye SY, Yang K (2014) A study of the temperature field during ultrasonic-assisted friction-stir welding. Int J Adv Manuf Technology 73: 321–327.
11. Tsujino J, Hidai K, Hasegawa A, Kanai R, Matsuura H, Matsushima K, Ueoka T (2002) Ultrasonic butt welding of aluminum, aluminum alloy and stainless steel plate specimens. Ultrasonic 40(1):371-374.
12.Tarasov SY, Rubtsov VE, Fortuna SV, Eliseev AA, Chumaevsky AV, Kalashnikova TA (2017) Ultrasonic-assisted aging in friction stir welding on Al-Cu-Li-Mg aluminum alloy. Weld World 61(4): 679–90.
13.Langenecker B (1996) Effects of ultrasound on deformation characteristics of metals. IEEE Trans Sonics Ultrasonic 13(1):1–8.
14.Park K, Kim GY, Ni J (2007) Design and analysis of ultrasonic assisted friction Stir welding. ASME.
15. Amini S, Rezaei A, Nazari M (2015) Bending vibrational tool for friction stir welding process. Int J Adv 84: 1–8.
16. Liu XC, Wu CS, Padhy GK (2015) Characterization of plastic deformation and material flow in ultrasonic vibration enhanced friction stir welding. Scr Mater 102:95-98.
17. Moradi MM, Aval HJ, Jamaati R (2017) Effect of Pre and Post welding heat treatment in SiC-fortified dissimilar AA6061-AA2024 FSW butt joint. J Manuf Proc, 30:97-105.
18.Kwanghyun Park (2009) Development and analysis of ultrasonic assisted Friction Stir Welding Process. Ph.D. thesis in the University of Michigan.
19.Zhong YB, Wu CS, Padhy GK(2017) Effect of ultrasonic vibration on welding load, temperature and material flow in friction stir welding. J Mat Proc Tech 239:279–83.
20. Ruilin L, Luocheng L, Diqiu H, Kunyu Y, Shaoyong Y(2014) A study of the temperature field during ultrasonic-assisted frictionstir welding. Int J Adv Manuf Tech 73:321–327.
21. Ji S, Huang R, Liu Z, Meng X (2017) Dissimilar friction stir welding of 6061 aluminum alloy and AZ31 magnesium alloy assisted with ultrasonic. Mater Lett 201:173–176.
22. Borigorla Venu, Raju LS, Venkata Rao K (2020) Multi objective optimization of friction stir weldments of AA2014-T651 by teaching–learning-based optimization. Proc IMechE Part C: J Mech Eng Sci 234(6):1146–1155.

23. Suvarna raju L, Borigorla venu (2020) Meta-heuristic optimization of copper friction stir weldments. Incas Bult 12(2): 163 – 171.
24. Kumar A, Suvarna Raju L (2012) Influence of Tool Pin Profiles on Friction Stir Welding of Copper. Mat and Manuf Proc 27(12): 1414-1418.
25. Hu Y, Liu H, Fujii H (2019) Improving the Mechanical characteristicsof 2219-T6 Al Alloy Weldments by Ultrasonic Vibrations during Friction Stir Welding. J Mat Proc Tech. 271:75-84.
26. Najib Muhammad A , Wu CS (2019) Ultrasonic vibration assisted friction stir welding of Al alloy and pure copper. J Manuf Proc 39: 114–127.
27. Liu XC, Wu CS(2013) Experimental Study on Ultrasonic Vibration Enhanced Friction Stir Welding. Proc of the 1st Int Joint Sym on Joining and Welding, Osaka, Japan, 6–8 November 2013:151-154.
28. Cheema MS, vivedi AD, Sharma AK(2013) A hybrid approach to multi-criteria optimization based on user's performance rating. proc Inst Mech Eng Part C J.Eng Manuf 227(11): 1733-1742.